Video Article

Whole-animal Imaging and Flow Cytometric Techniques for Analysis of Antigen-specific CD8+ T Cell Responses after Nanoparticle Vaccination

Lukasz J. Ochyl[1,2], James J Moon[1,2,3]

[1]Department of Pharmaceutical Sciences, University of Michigan

[2]Biointerfaces Institute, University of Michigan

[3]Department of Biomedical Engineering, University of Michigan

Correspondence to: James J Moon at moonjj@med.umich.edu

URL: https://www.jove.com/video/52771
DOI: doi:10.3791/52771

Keywords: Immunology, Issue 98, nanoparticle, vaccine, biomaterial, subunit antigen, adjuvant, cytotoxic CD8+ T lymphocyte, whole animal imaging, tetramer staining, and lymph node

Date Published: 4/29/2015

Citation: Ochyl, L.J., Moon, J.J. Whole-animal Imaging and Flow Cytometric Techniques for Analysis of Antigen-specific CD8+ T Cell Responses after Nanoparticle Vaccination. *J. Vis. Exp.* (98), e52771, doi:10.3791/52771 (2015).

Abstract

Traditional vaccine adjuvants, such as alum, elicit suboptimal CD8+ T cell responses. To address this major challenge in vaccine development, various nanoparticle systems have been engineered to mimic features of pathogens to improve antigen delivery to draining lymph nodes and increase antigen uptake by antigen-presenting cells, leading to new vaccine formulations optimized for induction of antigen-specific CD8+ T cell responses. In this article, we describe the synthesis of a “pathogen-mimicking” nanoparticle system, termed interbilayer-crosslinked multilamellar vesicles (ICMVs) that can serve as an effective vaccine carrier for co-delivery of subunit antigens and immunostimulatory agents and elicitation of potent cytotoxic CD8+ T lymphocyte (CTL) responses. We describe methods for characterizing hydrodynamic size and surface charge of vaccine nanoparticles with dynamic light scattering and zeta potential analyzer and present a confocal microscopy-based procedure to analyze nanoparticle-mediated antigen delivery to draining lymph nodes. Furthermore, we show a new bioluminescence whole-animal imaging technique utilizing adoptive transfer of luciferase-expressing, antigen-specific CD8+ T cells into recipient mice, followed by nanoparticle vaccination, which permits non-invasive interrogation of expansion and trafficking patterns of CTLs in real time. We also describe tetramer staining and flow cytometric analysis of peripheral blood mononuclear cells for longitudinal quantification of endogenous T cell responses in mice vaccinated with nanoparticles.

Video Link

The video component of this article can be found at https://www.jove.com/video/52771/

Introduction

Traditional vaccine development has mainly employed the empirical approach of trial-and-error. However, with the recent development of a wide array of biomaterials and discovery of molecular determinants of immune activation, it is now possible to rationally design vaccine formulations with biophysical and biochemical cues derived from pathogens[1,2]. In particular, various particulate drug delivery platforms have been examined as vaccine carriers as they can be co-loaded with subunit antigens and immunostimulatory agents, protect vaccine components from degradation, and enhance their co-delivery to antigen presenting cells (APCs) residing in lymph nodes (LNs), thus maximizing immune stimulation and activation[3-5]. In this report, we describe the synthesis of a “pathogen-mimicking” nanoparticle system, termed interbilayer-crosslinked multilamellar vesicles (ICMVs), which have been previously demonstrated as a potent vaccine platform for elicitation of robust cytotoxic T lymphocyte (CTL) and humoral immune responses in both systemic and mucosal tissue compartments[6-9]. In particular, vaccination with ICMVs achieved substantially enhanced serum IgG levels against a malaria antigen, compared with vaccination with conventional adjuvants (*e.g.,* alum and Montanide)[7] and also elicited potent CTL responses against tumor cells and viral challenge models in mice[9]. Here, using ICMVs as a model vaccine nanoparticle system, we describe methods for characterization of vaccine nano-formulations, including particle size and zeta potential measurements and tracking of particle trafficking to draining LNs (dLNs) utilizing confocal imaging of cryosectioned tissues[7]. In addition, we present a whole-animal imaging-based method of analyzing expansion of CTL responses in mice after adoptive transfer of luciferase-expressing antigen-specific CD8+ T cells[9,10]. Finally, we describe tetramer staining of peripheral blood mononuclear cells (PBMCs) for longitudinal quantification of endogenous T cell responses in mice vaccinated with nanoparticles[6,9].

ICMVs are a lipid-based nanoparticle formulation synthesized by controlled fusion of simple liposomes into multilamellar structures, which are then chemically stabilized by cross-linking maleimide-functionalized phospholipid head groups within lipid layers with dithiol crosslinkers[6]. Once ICMVs are synthesized, a small fraction of nanoparticles can be used to determine particle size and zeta potential (*i.e.,* surface charge of particles) with a dynamic light scattering (DLS) system and a zeta potential analyzer. DLS measures changes in light scattering in particle suspensions, allowing determination of the diffusion coefficient and the hydrodynamic size of particles[11]. Achieving consistent particle size from batch to batch synthesis is critical since particle size is one of the major factors influencing lymphatic draining of vaccine particles to dLNs and subsequent cellular uptake by APCs[12,13]. In addition, zeta potential can be obtained by measuring the particle velocity when an electric current is applied, which allows determination of the electrophoretic mobility of particles and particle surface charge[11]. Ensuring consistent

zeta potential values of particles is important since surface charge of particles determines colloidal stability, which has direct impact on particle dispersion during storage and after *in vivo* administration[14,15]. In order to track the particle localization to dLNs, ICMVs can be labeled with desired fluorophores including lipophilic dyes and covalently-tagged antigens. Following immunization, mice can be euthanized at various time points, dLNs resected, cryosectioned, and analyzed with confocal microscopy. This technique allows visualization of lymphatic draining of both the nanoparticle vaccine carriers and antigen to dLNs. The tissue sections can additionally be stained with fluorescently labeled antibodies and utilized to obtain more information, such as types of cells associated with the antigen and formation of germinal centers as we have shown previously[7].

Once the particle synthesis is optimized and trafficking to the dLNs is confirmed, it is important to validate elicitation of *in vivo* CTL expansion. In order to analyze elicitation of antigen-specific CD8+ T cells in response to nanoparticle vaccination, we have utilized a model antigen, ovalbumin (OVA), with $OVA_{257-264}$ peptide (SIINFEKL) immunodominant CD8+ T cell epitope, which allows detailed immunological analyses of antigen-specific T cell responses for initial vaccine development[16,17]. In particular, to interrogate the dynamics of expansion and migration of antigen-specific CD8+ T cells, we have generated a double-transgenic mouse model by crossing firefly luciferase-expressing transgenic mice (Luc) with OT-I transgenic mice that possess CD8+ T cells with T-cell receptor (TCR) specific for SIINFEKL (in association with $H\text{-}2K^b$). From these OT-I/Luc mice, luciferase-expressing, OT-I CD8+ T cells can be isolated and prepared for adoptive transfer into naïve C57BL/6 mice. Once seeded, successful immunization with OVA-containing nanoparticles will result in expansion of the transferred T cells, which can be tracked by monitoring the bioluminescence signal with a whole animal imaging system[9,10]. This non-invasive whole-body imaging technique has been used with other viral or tumor antigens in the past[18-20], revealing processes involved in T cell expansion in lymphoid tissues and dissemination to peripheral tissues in a longitudinal manner.

Complementary to analysis of adoptively transferred antigen-specific CD8+ T cells, endogenous T cell responses post vaccination can be examined with the peptide-major histocompatibility complex (MHC) tetramer assay[21], in which a peptide-MHC tetramer complex, consisting of four fluorophore-tagged MHC-class I molecules loaded with peptide epitopes, is employed to bind TCR and label CD8+ T cells in an antigen-specific manner. The peptide-MHC tetramer assay can be performed either in terminal necropsy studies to identify antigen-specific CD8+ T cells in lymphoid and peripheral tissues or in longitudinal studies with peripheral blood mononuclear cells (PBMCs) obtained from serial blood draws. After staining lymphocytes with peptide-MHC tetramer, flow cytometry analysis is performed for detailed analyses on the phenotype of CTLs or quantification of their frequency among CD8+ T cells.

Protocol

All experiments described in this protocol were approved by the University Committee on Use and Care of Animals (UCUCA) at University of Michigan and performed according to the established policies and guidelines.

1. Synthesis and Characterization of ICMVs Co-loaded with Protein Antigen and Adjuvant Molecules

1. Mix 1:1 molar ratio of 1,2-dioleoyl-*sn*-glycero-3-phosphocholine (DOPC) and 1,2-dioleoyl-*sn*-glycero-3-phosphoethanolamine-*N*-[4-(*p*-maleimidophenyl) butyramide] (MPB) in chloroform, keeping the total lipid amount at 1.26 µmol per batch (*i.e.,* 500 µg of DOPC and 630 µg of MPB) in a 20 ml glass vial (diameter = 28 mm and height = 61 mm).
2. Add lipophilic drugs, such as monophosphoryl lipid A (MPLA) or lipophilic dyes (*e.g.,* DiD), to the lipid solution at desired concentration. Thoroughly remove the organic solvent by purging with extra dry nitrogen gas and placing the samples under vacuum O/N.
3. Hydrate the lipid film by adding 200 µl of 10 mM bis-tris propane (BTP, pH 7.0) containing water-soluble drugs (*e.g.,* protein antigens). Vortex for 10 sec every 10 min for 1 hr at RT.
4. Transfer the contents from the glass vial into a 1.5 ml microcentrifuge tube, place samples in an ice-water bath, and sonicate continuously for 5 min using the 40% intensity setting on a 125 W/20 kHz probe-tip sonicator.
5. Add 4 µl of 150 mM dithiothreitol (DTT) to each batch (working concentration 2.4 mM), vortex, and briefly centrifuge using a tabletop microcentrifuge.
6. Add 40 µl of 200 mM $CaCl_2$ and mix with the pipette (working concentration 33 mM). Incubate samples at 37 °C for 1 hr to allow crosslinking of MPB-containing lipid layers with DTT.
7. Centrifuge samples at 20,000 x g for 15 min, remove the supernatant, and resuspend in 200 µl of $ddiH_2O$.
8. Repeat step 1.7 and centrifuge again after the second $ddiH_2O$ wash to remove $CaCl_2$, unreacted DTT, and unencapsulated cargo materials from the supernatant.
9. Prepare 10 mg/ml of 2 kDa polyethylene glycol-thiol (PEG-SH) in $ddiH_2O$. Resuspend each ICMV sample in 100 µl of PEG-SH solution and incubate at 37 °C for 30 min.
10. Perform two $ddiH_2O$ washes (step 1.7) and resuspend the final ICMV pellet in PBS and store at 4 °C. Prior to use, mix the ICMV suspension, as particles may settle to the bottom after prolonged storage.
11. For characterization of particles, remove a small aliquot (~10%) of ICMVs from each batch and dilute individually in a total volume of 1 ml of $ddiH_2O$. Place a single sample in a Zetasizer cell and measure particle size, polydispersity index, and zeta potential of the samples using a DLS and zeta potential measuring system (according to the manufacturer's protocol).

2. Examination of Lymph Node Draining of Fluorescence-tagged ICMVs with Confocal Microscopy

1. Preparation of ICMVs loaded with fluorophore-tagged antigen and lipophilic fluorescent dye
    1. Prepare fluorophore-tagged protein, such as ovalbumin reacted with Alexa Fluor 555-succinimidyl ester, according to the manufacturer's instruction.

2. To prepare ICMVs tagged with fluorophore in the lipid shell, add lipophilic fluorescent dye, (*e.g.,* 1,1′-Dioctadecyl-3,3,3′,3′-Tetramethylindodicarbocyanine, (DiD)) during preparation of the lipid film (Step 1.2) at 0.05% molar lipid amount. For lipid film hydration (Step 1.3), use buffer containing fluorophore-tagged antigen, and complete ICMV synthesis as outlined in steps 1.4-1.11.

2. Subcutaneous administration of nanoparticles at tail base
    1. Anesthetize mouse using a controlled flow vaporizer equipped with an induction chamber utilizing 3% isoflurane and 1.5 L/min of oxygen flow according to an IACUC approved animal protocol. Once the mouse is unconscious, perform the following steps quickly prior to the anesthesia wearing off to allow optimal access to the site of the injection and minimize discomfort to the animal. Alternatively, use a proper fitting nose cone to maintain anesthesia. If mice are anesthetized for longer than 5 min, apply eye lube necessary to minimize irritation after the procedure.
    2. Spray the base of the tail with 70% ethanol to sanitize and wet the fur Part the wet hair to expose a small patch of visible skin, which can be used to visualize the needle under the skin.
    3. Prepare particle injection suspension containing desired amount of antigen and adjuvant per 100 µl of vaccination dose in PBS (*e.g.,* 10 µg OVA and 0.3 µg MPLA per 100 µl of injection dose has been used in the past[6,9]).
    4. Draw the particle suspension into a syringe with a 27-29 G needle and insert the needle at the base of the tail (~5 mm from hairline) with the bevel facing up and inject 50 µl of the particle suspension[22].
    5. Wait a few seconds for pressure to equalize to prevent excessive back-flow and pull the needle out. Repeat the injection on the other side of the tail base to target both draining inguinal LNs.

3. Preparation of lymph node cryosections and examination with confocal microscopy.
    1. Euthanize the mouse with CO_2 asphyxiation, followed by induced pneumothorax according to an IACUC approved animal protocol. Extract inguinal LNs according to protocol demonstrated in Bedoya[23] and wash out the blood by placing the tissues in 1 ml of 4 °C PBS.
    2. Absorb the PBS from the tissues with tissues and place tissue in tissue cryomolds (10 x 10 x 5 mm^3) pre-filled to the top with OCT freezing medium[24]. Snap freeze the tissue block in liquid nitrogen for 30 sec. Alternatively, place tissue block on dry ice for 30 min. Store frozen tissue in -80 °C freezer.
    3. Cut tissue sections 5-10 µm thick in a cryostat set at -20 °C[24].
    4. If necessary, perform immunofluorescence labeling, and examine the tissue with confocal microscopy as previously demonstrated[24].

3. Monitoring Expansion of Antigen-specific, Luciferase-expressing CD8+ T Cells after Nanoparticle Vaccination with Whole Animal Imaging

1. Isolation of $OVA_{257-264}$-specific, luciferase-expressing CD8+ T cells from OT-I/Luc transgenic mice
    1. Euthanize an OT-I/Luc transgenic mouse with CO_2 asphyxiation and induce a pneumothorax according to an IACUC approved animal protocol. Harvest the spleen in a sterile manner by accessing the peritoneal cavity and carefully detaching the tissue from the pancreas[23], and place in 5 ml of 4 °C PBS + 2% FBS for transfer to tissue culture hood.
    2. Place the spleen on a 70 µm nylon strainer over a 50 ml conical centrifuge tube (up to 3 spleens at a time). Using a plunger from a 3 ml syringe, grind the cells through the strainer.
    3. Wash the plunger and the strainer with PBS + 2% FBS and discard. Bring the total volume to 10 ml/spleen in the 50 ml tube, take a small sample of the cell suspension to count with a hemocytometer, and centrifuge for 10 min at 300 x g.
    4. Using a commercially available magnetic negative selection kit, isolate the CD8+ T cell population by following the manufacturer's instructions.
    5. After washing cells with PBS, count the number of isolated CD8+ T cells. To assess purity of the isolated CD8+ T cells, incubate ~20,000-30,000 cells in 20 µl of mouse CD16/32 antibody (0.025 mg/ml) for 10 min, then add 20 µl of αCD8-APC antibody (0.005 mg/ml) and incubate for 30 min. Perform all incubations at 4 °C in PBS + 1% w/v BSA. Perform flow cytometric analysis[25].

2. Adoptive transfer of isolated CD8+ T cells and visualization of their expansion post vaccination
    1. Perform adoptive transfer of isolated OT-I/Luc CD8+ T cells into naïve C57BL/6 mice by administering 1-10 × 10^5 cells in a 200 µl volume of PBS via intravenous tail vein injection[22] (day -1). Considering that fur and black skin patches in C57BL/6 mice may interfere with the bioluminescent signal, shaved albino C57BL/6 mice are ideal for these studies.
    2. After one day (day 0), administer the vaccine as described previously (section 2.2).
    3. Administer 150 mg of luciferin per kg mouse body weight intraperitoneally in a 300 µl volume of PBS. After 10 min, anesthetize the mice with isoflurane (as in step 2.2.1) and visualize OT-I/Luc CD8+ T cells by acquiring the bioluminescence signal for 5-10 min with a whole animal imaging system (IVIS; refer to Wilson[26] for detailed instruction). Repeat as necessary for longitudinal studies.

4. Peptide-MHC Tetramer Staining of PBMCs for Analysis of Antigen-specific CD8+ T Cells

Note: The following protocol procedure can be performed using either C57BL/6 mice adoptively transferred with OT-I/Luc CD8+ T cells or C57BL/6 mice without the adoptive transfer.

1. At a desired time point after vaccination, collect approximately 100 µl of blood (4-6 drops) from mice via submandibular bleeding technique[27] into a tube coated with K_2EDTA and invert several times to prevent clotting.
2. Transfer 100 µl of blood to a microcentrifuge tube, add 1 ml of lysis buffer, and incubate for 2 to 3 min in order to remove red blood cells (RBCs). Centrifuge samples for 5 min at 1,500 x g and remove the supernatant. If the pellet still appears red (indicating incomplete removal of RBCs), repeat the lysis step with a brief incubation (< 1 min) of lysis buffer.
3. Wash the remaining PBMCs with 1 ml of FACS buffer (PBS + 1% w/v BSA) and centrifuge at 1,500 x g for 5 min.

4. Aspirate the supernatant and resuspend the sample in 20 µl of mouse CD16/32 antibody (0.025 mg/ml) to block nonspecific and FcR-mediated antibody binding. Incubate for 10 min at RT.
5. Transfer cells from microcentrifuge tubes into 4 ml round bottom FACS tubes. Add 20 µl of H-2K^b OVA Tetramer-SIINFEKL-PE solution according to the manufacturer's specifications to each sample and incubate for 30 min on ice.
6. Prepare the antibody cocktail (*e.g.,* αCD8-APC, αCD44-FITC, and αCD62L-PECy7 antibodies (0.005, 0.005, and 0.002 mg/ml concentration, respectively)). Add 20 µl to each experimental sample, and incubate for 20 min on ice. Prepare single fluorophore controls by labeling cells with each fluorophore-tagged tetramer or antibody at the concentration indicated above.
7. Wash 2 times with FACS buffer and resuspend the final pellet in FACS buffer containing 2 µg/ml of DAPI. The cells are now ready for flow cytometry analysis (details and examples can be found in Scheffold[25]).

Representative Results

The steps involved in the synthesis of ICMVs are illustrated in **Figure 1**[6]. Briefly, a lipid film containing any lipophilic drugs or fluorescent dyes is hydrated in the presence of hydrophilic drugs. Divalent cations, such as Ca^{2+}, are added to drive fusion of anionic liposomes into multilamellar vesicles. Dithiol crosslinker, such as DTT, is added to "staple" maleimide-functionalized lipids on apposing lipid layers, and finally remaining external maleimide groups are quenched in a reaction with thiolated-PEG moieties. A small fraction of each batch can be readily subjected to quality control measurements by determining particle size, polydispersity index, and zeta potential with a DLS and zeta potential analysis system. The resulting particles are relatively homogenous with an average size of 130 ± 20 nm, polydispersity index of 0.22 ± 0.02, and zeta potential of -54 ± 3 mV for OVA-encapsulating particles (**Figure 1B and 1C**). Typical yield of particles, measured in dry weight of particles, is ~50%[6].

Using the protocol described above, ICMVs can be co-loaded with fluorophore-tagged protein antigen and fluorescent lipophilic dye, allowing visualization of antigen and nanoparticle delivery *in vivo*. To compare the patterns of antigen delivery in soluble form versus in ICMVs, C57BL/6 mice were administered s.c. at tail base with 100 µg of AlexaFluor555-tagged OVA either in soluble or DiD-labeled ICMV formulations, and draining inguinal LNs were excised at various time points for preparation of dLN tissue cryo-sections. Visualization with confocal microscopy indicated that soluble antigen quickly reached the dLNs within 4 hr, but was also cleared very rapidly with 24 hr (**Figure 2**)[7]. In contrast, OVA-loaded ICMVs were detected at the periphery of dLNs by 24 hr, with continued accumulation as examined on day 4, depositing a large amount of OVA-ICMVs in dLNs (**Figure 2**). Confocal micrographs also showed co-localization of AlexaFluor555-tagged OVA and DiD-labeled ICMVs within dLNs, suggesting that ICMVs permit stable co-delivery of protein antigens and other immunostimulatory agents encapsulated within ICMVs[7].

Isolation of CD8+ T cells from OT-I/Luc transgenic mouse can be readily performed with the commercially available magnetic negative selection kit, yielding ~ 8-12 x 10^6 cells per a mouse spleen. **Figure 3** shows C57BL/6 mice adoptively transferred with 5 x 10^5 OT-I/Luc CD8+ T cells on day -1, and immunized on day 0 with s.c. administration of 10 µg of OVA and 0.3 µg of MPLA either in soluble or ICMV formulations. Bioluminescence imaging with IVIS performed on day 0 prior to vaccination showed minimal OT-I/Luc signal. However, by day 4 post vaccination, mice immunized with OVA/MPLA-ICMVs had robust bioluminescence signal within inguinal LNs, which are LNs draining the tail base region[28]. In contrast, mice immunized with the soluble form of the vaccine showed much reduced expansion of OT-I/Luc CD8+ T cells within inguinal dLNs.

Using OVA as a model antigen allows monitoring of expansion of endogenous CD8+ T cells specific to immunodominant $OVA_{257-264}$ peptide (SIINFEKL). For example, C57BL/6 mice were immunized on days 0, 21, and 35 with s.c. administration of 10 µg OVA and 0.3 µg MPLA in either ICMVs or soluble form, and frequencies of SIINFEKL-specific CD8+ T cells among CD8+ T cells in PBMCs were determined by flow cytometric analysis of PBMCs stained with SIINFEKL-H-2K^b tetramer-PE. **Figure 4A** shows representative flow cytometry scatter plots of SIINFEKL-H-2K^b tetramer$^+$ cells among CD8+ T cells in PBMCs on day 41[6]. **Figure 4B** shows representative scatter plots of CD62L+CD44+ cells with central memory phenotype among SIINFEKL-tetramer+ CD8+ T cells. Weekly monitoring of PBMCs shown in **Figure 4C** indicated that soluble OVA vaccine elicited minimal expansion of antigen-specific CD8+ T cells, whereas ICMV vaccination elicited significantly stronger CD8$^+$ T cell responses, achieving a peak 28% SIINFEKL-tetramer$^+$ T cells in the CD8$^+$ T cell population by day 41[6]. Using the tetramer staining protocol presented here, we observed the background frequency of 0.11% ± 0.04% OVA-specific T cells (N = 15) in untreated or PBS-treated animals, and we can detect statistically significant increase in antigen-specific CD8+ T cell frequencies as low as 0.46% ± 0.05% (p-value < 0.005, data not shown).

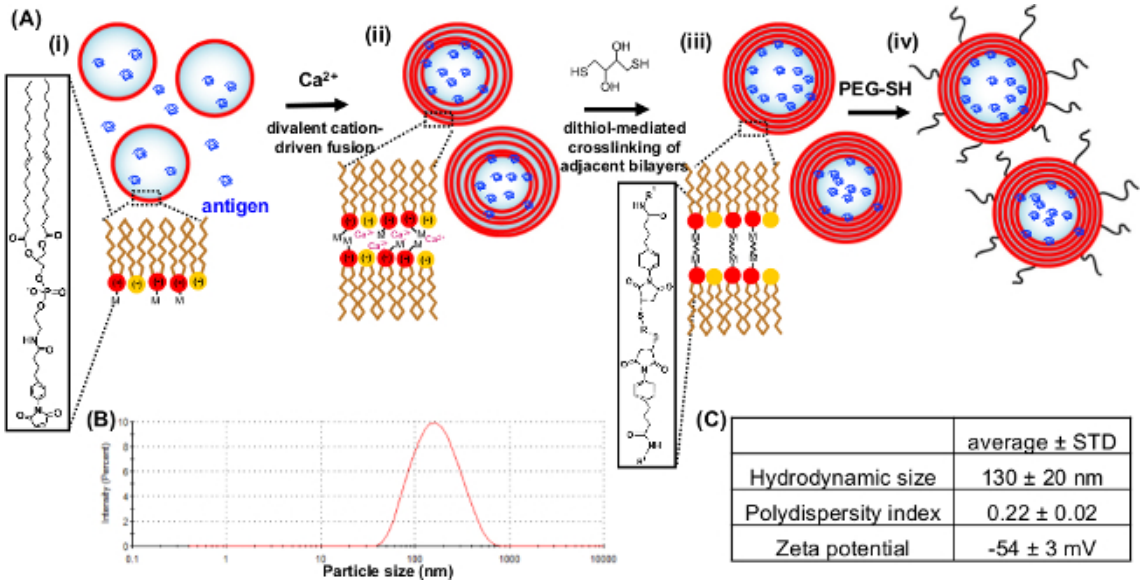

Figure 1. Synthesis and characterization of interbilayer-crosslinked multilamellar vesicles (ICMVs). (**A**) ICMVs are synthesized in the following 4 steps; (i) anionic, maleimide-functionalized liposomes are prepared from dried lipid films; (ii) divalent cations are added to induce fusion of liposomes and the formation of multilamellar vesicles; (iii) membrane-permeable dithiols are added, which crosslink maleimide-lipids on apposed lipid bilayers in the vesicle walls; and (iv) the resulting lipid particles are PEGylated with thiol-terminated PEG. (**B**) Representative particle distribution as analyzed by DLS is shown. (**C**) Average hydrodynamic size, polydispersity index, and zeta potential of ICMVs co-loaded with OVA and MPLA are shown. Panel (A) has been modified from Moon *et al.*[6]. Please click here to view a larger version of the figure.

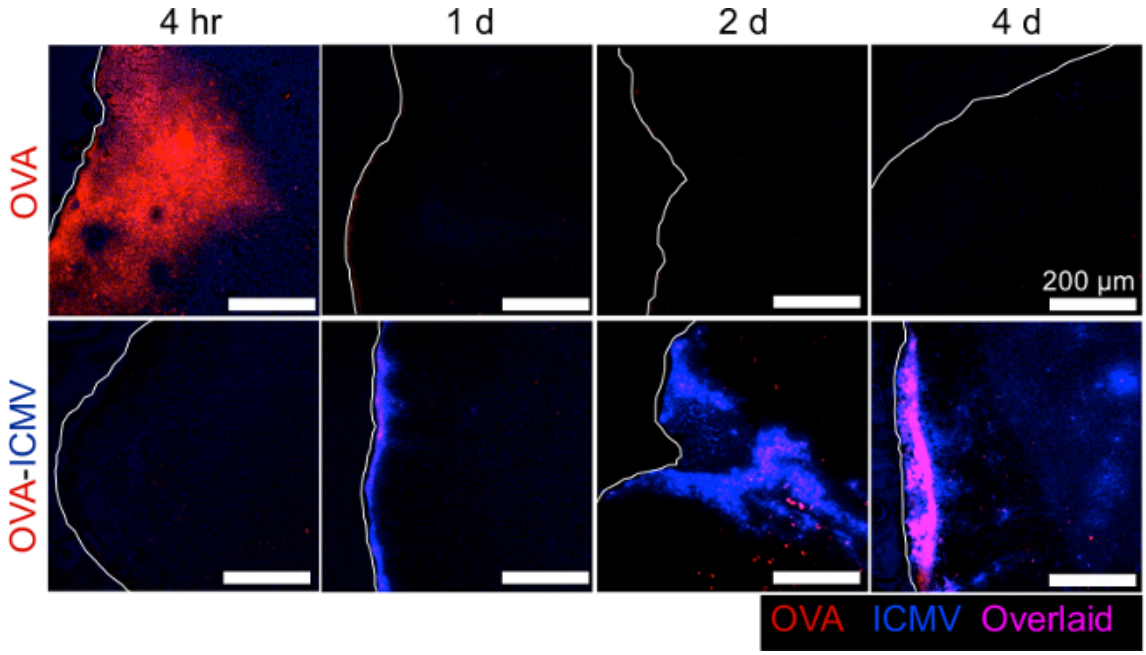

Figure 2. Analysis of antigen draining to lymph nodes with confocal microscopy. C57Bl/6 mice were immunized with 100 μg fluorophore-conjugated OVA (shown in red) and 5 μg MPLA either in solution or ICMVs (shown in blue). Draining inguinal lymph nodes were excised at indicated time points, cryosectioned, and imaged with confocal microscopy. Representative confocal micrographs are shown. Pink signals indicate co-localization of OVA and ICMVs. This figure has been modified from Moon *et al.*[7]. Please click here to view a larger version of this figure.

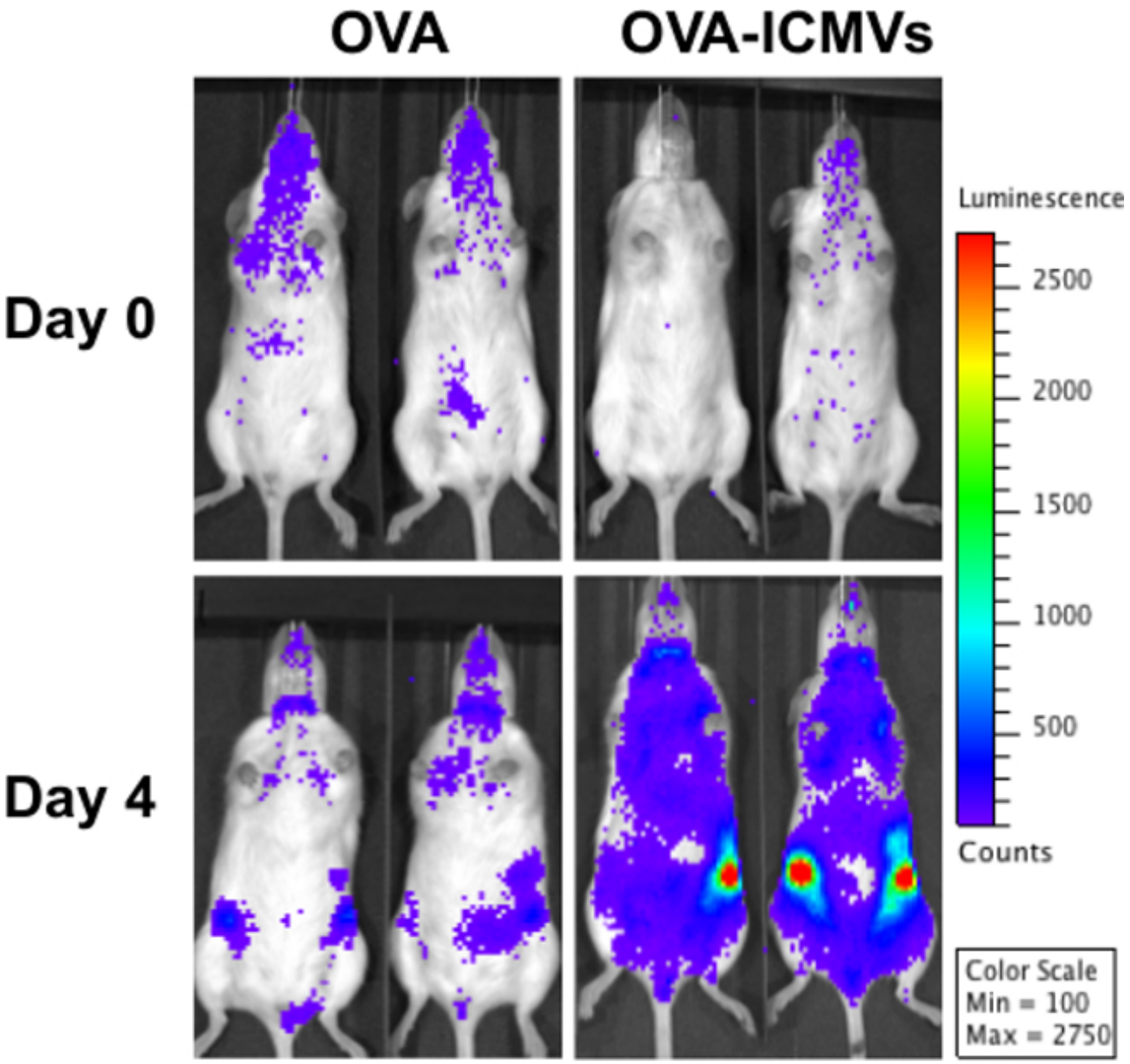

Figure 3. Monitoring T cell expansion after vaccination. C57Bl/6 albino mice were adoptively transferred i.v. with 5 x 10^5 Luc^+ OT-I $CD8^+$ T cells on day -1. On day 0, the animals were administered with 10 µg of OVA and 0.1 µg of MPLA either as soluble or ICMV formulations. The animals were anesthetized with isoflurane and administered with luciferin (150 mg/kg, 300 µl injected i.p.), and bioluminescence signal from Luc^+OT-1 $CD8^+$ T cells was acquired with IVIS. Please click here to view a larger version of this figure.

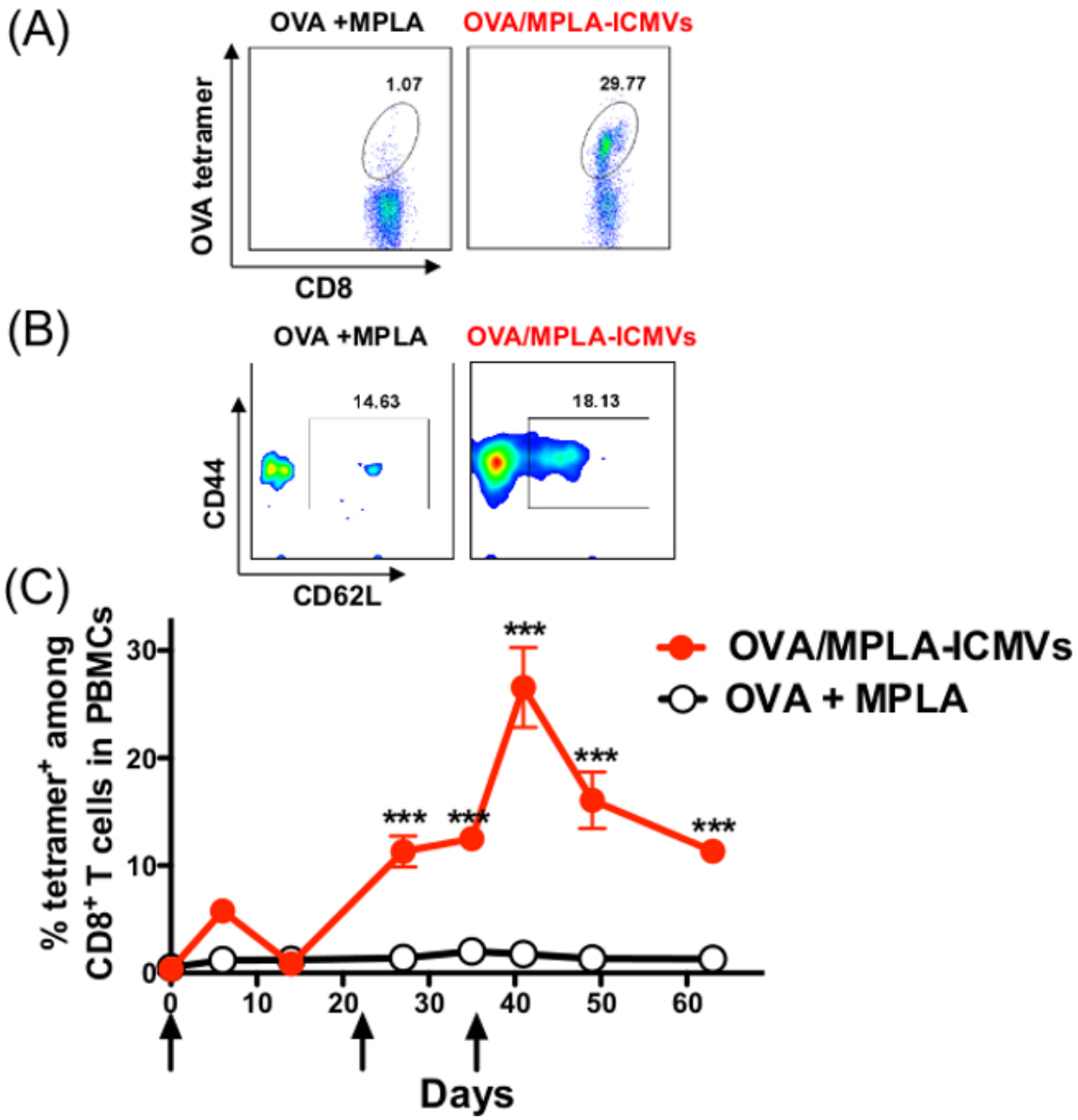

Figure 4. Expansion of endogenous OVA-specific CD8+ T cells after ICMV vaccination. C57Bl/6 mice were immunized with 10 µg of OVA and 0.1 µg of MPLA either in solution or ICMVs on days 0, 21, and 35 (arrows). Frequency of OVA-specific T cells among peripheral blood mononuclear cells was assessed over time by flow cytometric analysis of SIINFEKL-MHC-I tetramer$^+$ CD8+ T cells. (**A**) Representative flow cytometry scatter plots from individual mice at day 41 show SIINFEKL-MHC-I tetramer$^+$ CD8+ T cells and (**B**) CD62L+CD44+ cells, marker of central memory T cells. (**C**) The overall kinetics of T cell expansion and contraction is shown. This figure has been modified from Moon *et al.*[6]. Please click here to view a larger version of the figure.

Discussion

The protocol provided in this article describes the synthesis and characterization of a new lipid-based nanoparticle system, termed ICMVs, and provides the process of validating effectiveness of nanoparticle-based vaccine formulations to induce antigen-specific CD8+ T cell responses. ICMV synthesis is completed in all aqueous condition, which is a major advantage compared with other commonly used polymeric nanoparticle systems (*e.g.*, poly(lactide-co-glycolide) acid particles), which typically require organic solvents for preparation, often resulting in loss of antigenicity in protein antigens[29,30]. In addition, ICMVs benefit from extensive stability and capability to encapsulate both hydrophobic and hydrophilic molecules[6], thus permitting co-delivery of antigens and adjuvants targeted to the same intracellular compartment within APCs[31,32]. Using ICMVs as a model vaccine nanoparticle, here we have outlined the procedures for (1) nanoparticle synthesis and characterization, (2) validation of nanoparticle drainage to dLNs, and examination of elicitation of antigen-specific CD8+ T cell responses using (3) a non-invasive bioluminescence imaging technique and (4) the peptide-MHC tetramer staining assay on PBMCs.

It is critical to ensure uniformity in nanoparticle synthesis from batch to batch, especially for particle size and surface charge as they can greatly affect lymphatic draining and uptake by APCs upon *in vivo* administration. DLS and zeta potential analysis provide quick methods of quality check on particle size and surface charge. For more detailed analyses on morphology of individual particles, these techniques can be complemented with high-resolution electron microscopy, such as cryo-electron microscopy (cryo-EM) that preserves morphology of “soft”

particles in vitrified aqueous layer[6,33,34]. Encapsulation efficiency of antigens and adjuvants must also be determined and kept uniform between syntheses. Adjuvants, such as MPLA, can be tagged with a fluorophore[6] whereas protein antigens can be quantified using absorbance- and fluorescence-based protein quantification kits, or analyzed utilizing SDS-PAGE[35] and Coomassie or silver staining[36], and quantified based on band intensity. Inconsistencies in particle preparation may result from expired or poorly-stored reagents, as optimal reactivity is necessary for complete synthesis. To this end, maleimide- and thiol- functionalized reagents should be kept in small aliquots at -80 °C without frequent freeze-thaw cycles.

Particles smaller than 100 nm are generally thought to effectively enter the lymphatic vessels and traffic to dLNs[13], whereas larger particles (500-2,000 nm) require active transport by tissue-resident DCs[12,37]. In our hands, ICMVs with the hydrodynamic size ranging from 150-250 nm efficiently localized and persisted in the dLN, resulting in extensive CTL and humoral responses[6,7]. Within 24 hr of administration, ICMVs were associated with subcapsular sinus macrophages in dLNs, and flow cytometric analyses performed on days 1 and 4 indicated that most ICMVs within dLNs were taken up by LN-resident APCs with only a small portion of particles associated with Langerhans and dermal DCs[7]. These results indicated that passive transport is the major mode of ICMV trafficking to dLNs. These studies have utilized fluorophore-tagged nanoparticles and protein antigens to delineate their localization and distribution patterns in dLNs. Confocal microscopy of cryosectioned dLNs allows additional immunofluorescence histochemistry for identification of LN structures (*e.g.*, GL-7 expression in germinal centers) and cells interacting with the formulation components (*e.g.*, DCs – CD11c, macrophages – F4/80, CD169, and B-cells – B220)[7,9]. This technique can be performed in parallel with flow cytometry analyses of cells harvested from dLNs to delineate the subsets of APCs responsible for particle uptake[7,9] or with whole-animal imaging to quantitate vaccine delivery from injection site to dLNs[38,39], provided that the fluorescent signals are strong and tissue autofluorescence does not interfere with the signals.

Effective immunization requires robust activation and expansion of antigen-specific cytotoxic T cells, which can be tracked by whole-body bioluminescence imaging after adoptive transfer of bioluminescent, antigen-specific transgenic T cells, followed by vaccination. The added benefit of this method is the potential for repeated visualization of CTL trafficking in the same animals for an extended period, thus reducing the number of animals required for immunological analyses and avoiding the use of laborious cell isolation procedures. Using this imaging technique, we have recently demonstrated that pulmonary administration of ICMVs co-loaded with protein antigen and an immunostimulatory agent led to potent elicitation of antigen-specific CD8+ T cells in the lung and mediastinal LNs and subsequent dissemination of CTLs to distal mucosal tissues, including Peyer's patches, cecum, and vaginal tract[9]. Flow cytometric analyses showed that these newly expanded CD8+ T cells were imprinted with a "mucosal-homing" phenotype characterized by $\alpha_4\beta_7^+$ integrin expression and mediated protective immune responses against mucosal viral challenge[9]. The whole-animal imaging of bioluminescent CD8+ T cells was also recently utilized by Hailemicheal *et al*., who demonstrated that tumor antigen peptide formulated into incomplete Freund's adjuvant (IFA, oil-in-water emulsion) resulted in sequestration of T cells at the site of the injection with vaccine "depot" away from the tumor masses, leading to T cell dysfunction and deletion[40].

Tetramer staining has been used extensively in the past to quantify the level of endogenous CTL responses resulting from various vaccine formulations[21]. This technique is also relevant and commonly utilized in early human cancer immunotherapy clinical trials to confirm CTL responses to specific tumor-associated antigens[41,42]. PBMCs can be easily collected from mice and prepared for flow cytometry; however, it may not reveal the full extent of T-cell expansion due to cell localization to depot-forming vaccines as mentioned before or within tumors in cancer models, thus requiring more extensive analysis. Compatibility of this method with flow cytometry allows determination of antigen-specific T cells with memory markers (CD44, CD62L, CD127, Bcl-2, and KLRG-1) to distinguish effector, central memory, and effector memory cells among the tetramer+ T cells[43] or long-lasting tissue resident CTLs[44,45] (as summarized in recent reviews [46,47]). However, the tetramer staining assay provides only the initial assessment of CTL responses since highly-expanded antigen-specific T cells may exhibit signs of immune exhaustion[48,49]. Functional evaluation of CTL responses can be performed by examining cytokine release with enzyme linked immunospot (ELISpot)[50] or intracellular cytokine staining[51] after *ex vivo* stimulation of lymphocytes with minimal epitopes as well as by measuring the intracellular levels of perforin and granzyme B[52] and extracellular expression of CD107a and CD107b upon degranulation[53]. In addition, cytolytic function of CTLs can be directly assessed with CTL cytotoxicity assays performed *in vitro* or *in vivo*[54-56].

Induction of humoral immune responses after nanoparticle vaccination can be studied in parallel with the CD8+ T cell analyses presented here. Antibody titers can be analyzed by the traditional method of enzyme-linked immunosorbent assay (ELISA) while antibody affinity and breadth of epitope recognition can be assessed by modifying the ELISA protocol with the use of chaotropic agent (*e.g.,* urea) during antibody binding to the substrate and the use of subdomains within antigens as substrates, respectively[7]. Elicitation of potent humoral responses requires expansion of follicular helper CD4+ T cells (T_{fh})[57]. To investigate expansion of T_{fh} cells in response to particle vaccination, the protocol presented here can be readily adapted for isolation of antigen-specific CD4+ T cells from OT-II transgenic mice, followed by adoptive cell transfer into naïve recipient mice. After vaccination, lymphoid tissues can be harvested and analyzed with flow cytometric analyses to determine expansion of antigen-specific T_{fh} cells (identified by their CD4+CXCR5+PD-1+ phenotype)[7].

Disclosures

Perkin Elmer provided the production cost incurred during the publication of this article.

Acknowledgements

This study was supported by the National Institute of Health grant 1K22AI097291-01 and by the National Center for Advancing Translational Sciences of the National Institutes of Health under Award Number UL1TR000433. We also acknowledge Prof. Darrell Irvine at MIT and Prof. Matthias Stephan at Fred Hutchinson Cancer Center for their contribution on the initial work on the vaccine nanoparticles and OT-I/Luc transgenic mice.

References

1. Irvine, D. J., Swartz, M. A., Szeto, G. L. Engineering synthetic vaccines using cues from natural immunity. *Nature materials.* **12**, 978-990 (2013).
2. Moon, J. J., Huang, B., Irvine, D. J. Engineering nano- and microparticles to tune immunity. *Advanced materials.* **24**, 3724-3746 (2012).
3. Sahdev, P., Ochyl, L. J., Moon, J. J. Biomaterials for nanoparticle vaccine delivery systems. *Pharmaceutical Research.* (2014).
4. Zhao, L., *et al.* Nanoparticle vaccines. *Vaccine.* **32**, 327-337 (2014).
5. Riet, E., Ainai, A., Suzuki, T., Kersten, G., Hasegawa, H. Combatting infectious diseases; nanotechnology as a platform for rational vaccine design. *Advanced drug delivery reviews.* **74C**, 28-34 (2014).
6. Moon, J. J., *et al.* Interbilayer-crosslinked multilamellar vesicles as synthetic vaccines for potent humoral and cellular immune responses. *Nature Materials.* **10**, 243-251 (2011).
7. Moon, J. J., *et al.* Enhancing humoral responses to a malaria antigen with nanoparticle vaccines that expand Tfh cells and promote germinal center induction. *Proceedings of the National Academy of Sciences of the United States of America.* **109**, 1080-1085 (2012).
8. DeMuth, P. C., Moon, J. J., Suh, H., Hammond, P. T., Irvine, D. J. Releasable layer-by-layer assembly of stabilized lipid nanocapsules on microneedles for enhanced transcutaneous vaccine delivery. *ACS Nano.* **6**, 8041-8051 (2012).
9. Li, A. V., *et al.* Generation of Effector Memory T Cell-Based Mucosal and Systemic Immunity with Pulmonary Nanoparticle Vaccination. *Science Translational Medicine.* **5**, 204ra130 (2013).
10. Stephan, M. T., Moon, J. J., Um, S. H., Bershteyn, A., Irvine, D. J. Therapeutic cell engineering with surface-conjugated synthetic nanoparticles. *Nature Medicine.* **16**, 1035-1041 (2010).
11. Murdock, R. C., Braydich-Stolle, L., Schrand, A. M., Schlager, J. J., Hussain, S. M. Characterization of nanomaterial dispersion in solution prior to In vitro exposure using dynamic light scattering technique. *Toxicological Sciences.* **101**, 239-253 (2008).
12. Manolova, V., *et al.* Nanoparticles target distinct dendritic cell populations according to their size. *European Journal of Immunology.* **38**, 1404-1413 (2008).
13. Reddy, S. T., *et al.* Exploiting lymphatic transport and complement activation in nanoparticle vaccines. *Nature Biotechnology.* **25**, 1159-1164 (2007).
14. Kaur, R., Bramwell, V. W., Kirby, D. J., Perrie, Y. Manipulation of the surface pegylation in combination with reduced vesicle size of cationic liposomal adjuvants modifies their clearance kinetics from the injection site, and the rate and type of T cell response. *Journal of Controlled Release.* **164**, 331-337 (2012).
15. Zhuang, Y., *et al.* PEGylated cationic liposomes robustly augment vaccine-induced immune responses: Role of lymphatic trafficking and biodistribution. *Journal of Controlled Release.* **159**, 135-142 (2012).
16. Hogquist, K. A., *et al.* T cell receptor antagonist peptides induce positive selection. *Cell.* **76**, 17-27 (1994).
17. Clarke, S. R. M., *et al.* Characterization of the ovalbumin-specific TCR transgenic line OT-I: MHC elements for positive and negative selection. *Immunology and Cell Biology.* **78**, 110-117 (2000).
18. Azadniv, M., Dugger, K., Bowers, W. J., Weaver, C., Crispe, I. N. Imaging CD8(+) T cell dynamics in vivo using a transgenic luciferase reporter. *International Immunology.* **19**, 1165-1173 (2007).
19. Kim, D., Hung, C. F., Wu, T. C. Monitoring the trafficking of adoptively transferred antigen- specific CD8-positive T cells in vivo, using noninvasive luminescence imaging. *Human gene therapy.* **18**, 575-588 (2007).
20. Rabinovich, B. A., *et al.* Visualizing fewer than 10 mouse T cells with an enhanced firefly luciferase in immunocompetent mouse models of cancer. *Proceedings of the National Academy of Sciences of the United States of America.* **105**, 14342-14346 (2008).
21. Altman, J. D., *et al.* Phenotypic analysis of antigen-specific T lymphocytes. *Science.* **274**, 94-96 (1996).
22. Machholz, E., Mulder, G., Ruiz, C., Corning, B. F., Pritchett-Corning, K. R. Manual Restraint and Common Compound Administration Routes in Mice and Rats. *Journal of Visualized Experiments.* e2771 (2012).
23. Bedoya, S. K., Wilson, T. D., Collins, E. L., Lau, K., Larkin Iii, J. Isolation and Th17 Differentiation of Naive CD4 T Lymphocytes. *Journal of Visualized Experiments.* e50765 (2013).
24. Chen, Y., *et al.* Visualization of the interstitial cells of cajal (ICC) network in mice. *Journal of Visualized Experiments.* (2011).
25. Scheffold, A., Busch, D. H., Kern, F. In Cellular Diagnostics Basics, Methods and Clinical Applications of Flow Cytometry. *Karger.* Sack, U., Tárnok, D. H., Rothe, G. 476-502 (2009).
26. Wilson, K., Yu, J., Lee, A., Wu, J. C. In vitro and in vivo Bioluminescence Reporter Gene Imaging of Human Embryonic Stem Cells. *Journal of Visualized Experiments.* e740 (2008).
27. Golde, W. T., Gollobin, P., Rodriguez, L. L. A rapid, simple, and humane method for submandibular bleeding of mice using a lancet. *Lab Animal.* **34**, 39-43 (2005).
28. Tilney, N. L. Patterns of lymphatic drainage in the adult laboratory rat. *Journal of Anatomy.* **109**, 369-383 (1971).
29. Stivaktakis, N., *et al.* PLA and PLGA microspheres of beta-galactosidase: Effect of formulation factors on protein antigenicity and immunogenicity. *Journal of Biomedical Materials Research Part A.* **70A**, 139-148 (2004).
30. Bilati, U., Allemann, E., Doelker, E. Nanoprecipitation versus emulsion-based techniques for the encapsulation of proteins into biodegradable nanoparticles and process-related stability issues. *AAPS PharmSciTech.* **6**, E594-E604 (2005).
31. Blander, J. M., Medzhitov, R. Toll-dependent selection of microbial antigens for presentation by dendritic cells. *Nature.* **440**, 808-812 (2006).
32. Iwasaki, A., Medzhitov, R. Regulation of adaptive immunity by the innate immune system. *Science.* **327**, 291-295 (2010).
33. Dubochet, J., *et al.* Cryo-electron microscopy of vitrified specimens. *Quarterly reviews of biophysics.* **21**, 129-228 (1988).
34. Vinson, P. K., Talmon, Y., Walter, A. Vesicle-micelle transition of phosphatidylcholine and octyl glucoside elucidated by cryo-transmission electron microscopy. *Biophysical Journal.* **56**, 669-681 (1989).
35. Schagger, H. Tricine-SDS-PAGE. *Nature Protocols.* **1**, 16-22 (2006).
36. Chevallet, M., Luche, S., Rabilloud, T. Silver staining of proteins in polyacrylamide gels. *Nat Protoc.* **1**, 1852-1858 (2006).
37. Randolph, G. J., Angeli, V., Swartz, M. A. Dendritic-cell trafficking to lymph nodes through lymphatic vessels. *Nature Reviews Immunology.* **5**, 617-628 (2005).
38. Liu, H., *et al.* Structure-based programming of lymph-node targeting in molecular vaccines. *Nature.* **507**, 519-522 (2014).

39. Xu, Z., *et al.* Multifunctional nanoparticles co-delivering Trp2 peptide and CpG adjuvant induce potent cytotoxic T-lymphocyte response against melanoma and its lung metastasis. *Journal of Controlled Release.* **172**, 259-265 (2013).
40. Hailemichael, Y., *et al.* Persistent antigen at vaccination sites induces tumor-specific CD8(+) T cell sequestration, dysfunction and deletion. *Nature Medicine.* **19**, 465 (2013).
41. Slingluff, C. L., *et al.* Phase I trial of a melanoma vaccine with gp100(280-288) peptide and tetanus helper peptide in adjuvant: Immunologic and clinical outcomes. *Clinical Cancer Research.* **7**, 3012-3024 (2001).
42. Speiser, D. E., *et al.* Rapid and strong human CD8(+) T cell responses to vaccination with peptide, IFA, and CpG oligodeoxynucleotide 7909. *Journal of Clinical Investigation.* **115**, 739-746 (2005).
43. Araki, K., *et al.* mTOR regulates memory CD8 T-cell differentiation. *Nature.* **460**, 108-112 (2009).
44. Masopust, D., Vezys, V., Marzo, A. L., Lefrancois, L. Preferential localization of effector memory cells in nonlymphoid tissue. *Science.* **291**, 2413-2417 (2001).
45. Cuburu, N., *et al.* Intravaginal immunization with HPV vectors induces tissue-resident CD8+ T cell responses. *Journal of Clinical Investigation.* **122**, 4606-4620 (2012).
46. Ahlers, J. D., Belyakov, I. M. Memories that last forever: strategies for optimizing vaccine T-cell memory. *Blood.* **115**, 1678-1689 (2010).
47. Seder, R. A., Darrah, P. A., Roederer, M. T-cell quality in memory and protection: implications for vaccine design. *Nature Reviews Immunology.* **8**, 247-258 (2008).
48. Barber, D. L., *et al.* Restoring function in exhausted CD8 T cells during chronic viral infection. *Nature.* **439**, 682-687 (2006).
49. Wherry, E. J., *et al.* Molecular signature of CD8+ T cell exhaustion during chronic viral infection. *Immunity.* **27**, 670-684 (2007).
50. Czerkinsky, C. C., Nilsson, L. A., Nygren, H., Ouchterlony, O., Tarkowski, A. A solid-phase enzyme-linked immunospot (ELISPOT) assay for enumeration of specific antibody-secreting cells. *Journal of Immunological Methods.* **65**, 109-121 (1983).
51. Foster, B., Prussin, C., Liu, F., Whitmire, J. K., Whitton, J. L. Detection of intracellular cytokines by flow cytometry. *Current Protocols in Immunology.* **Chapter 6**, (Unit 6 24), (2007).
52. Wonderlich, J., Shearer, G., Livingstone, A., Brooks, A. Induction and measurement of cytotoxic T lymphocyte activity. *Current protocols in immunology.* **Chapter 3**, (Unit 6 24), (2006).
53. Betts, M. R., *et al.* Sensitive and viable identification of antigen-specific CD8+T cells by a flow cytometric assay for degranulation. *Journal of Immunological Methods.* **281**, 65-78 (2003).
54. Brunner, K. T., Mauel, J., Cerottini, J. C., Chapuis, B. Quantitative assay of the lytic action of immune lymphoid cells on 51-Cr-labelled allogeneic target cells in vitro; inhibition by isoantibody and by drugs. *Immunology.* **14**, 181-196 (1968).
55. Noto, A., Ngauv, P., Trautmann, L. Cell-based flow cytometry assay to measure cytotoxic activity. *Journal of Visualized Experiments.* e51105 (2013).
56. Quah, B. J., Wijesundara, D. K., Ranasinghe, C., Parish, C. R. The use of fluorescent target arrays for assessment of T cell responses in vivo. *Journal of visualized experiments.* e51627 (2014).
57. Crotty, S. Follicular helper CD4 T cells (TFH). *Annual review of immunology.* **29**, 621-663 (2011).

